Research Article

Massimo Beltrame*, Simona Rafanelli, Costanza Quaratesi, José Mirão, Ginevra Coradeschi

Roof Tiles and Bricks of the Etruscan *Domus dei Dolia* (*Vetulonia*, Italy): An Archaeological and Archaeometric Study of Construction Materials

https://doi.org/10.1515/opar-2022-0322
received March 31, 2023; accepted June 23, 2023

Abstract: In this article, the archaeological and archaeometrical study of several roof tiles and bricks retrieved at the Etruscan *Domus dei Dolia* is presented. The *Domus* is located in Etrusco-Roman neighbourhood (Hellenistic – Late Republican periods, third–first centuries BC) of the ancient city of *Vetulonia* (central Italy), in the area of *Poggiarello Renzetti*. The main goals were to establish the characteristics of the raw material/s used in their production, the possible provenance, the technology applied, and to get insight regarding the production organization and the local economy. The archaeological materials were analysed by optical microscopy (OM), X-ray diffraction (XRD), and X-ray fluorescence (XRF). Principal component analysis was also applied to evaluate/interpret chemical data. Results evidenced that roof tiles and bricks were produced using a different technology and raw materials. Roof tiles were possibly manufactured within 12 km from the archaeological site and imported into the town, exploiting two different raw materials. Conversely, bricks were likely produced very close to the archaeological site. So, it is supposed that raw materials were selected considering factors such as distance, abundance, and accessibility to natural resources and security.

Keywords: Etruscan, Southern Tuscany, roof tiles, bricks, raw materials

1 Introduction

Etruscans were one of the most important and sophisticated ancient Italian civilization before the rise of Rome (Ceccarelli, 2016; Neil, 2016; Stoddart, 2016), and they had a great cultural impact on the Roman civilization. Known as *Tyrsenoi* or *Thyrrenoi* by ancient Greeks, Etruscan people ruled in the Italian Peninsula between the ninth and the first century BC. Their presence has been attested in different regions of central Italy such as

Special Issue on Bricks Under the Scope: Microscopic and Macroscopic Approaches to the Study of Earthen Architecture, edited by Marta Lorenzon, Moritz Kinzel, & Benjamín Cutillas-Victoria.

*** Corresponding author: Massimo Beltrame**, HERCULES Laboratory, Associated Laboratory in2Past, City University of Macau Chair on Sustainable Heritage of the University of Évora, Pálacio do Vimioso, Largo Marquês de Marialva 8, 7000-809 Évora, Portugal, e-mail: massimo@uevora.pt
Simona Rafanelli, Costanza Quaratesi: Isidoro Falchi Civic Archaeological Museum, Piazza Vetluna, Vetulonia, 58043, Italy
José Mirão: HERCULES Laboratory, Associated Laboratory in2Past, City University of Macau Chair on Sustainable Heritage, Geoscience Department of the University of Évora, Pálacio do Vimioso, Largo Marquês de Marialva 8, 7000-809 Évora, Portugal
Ginevra Coradeschi: HERCULES Laboratory, Associated Laboratory in2Past, City University of Macau Chair on Sustainable Heritage of the University of Évora, Pálacio do Vimioso, Largo Marquês de Marialva 8, 7000-809 Évora, Portugal

Tuscany, Lazio, Umbria, Campania, in large areas of the Po Valley (Emilia Romagna, Lombardia, and Veneto regions) in northern Italy, and in the Corsica Island (France) (Cristofani, 2000). According to ancient sources, they are considered to have been organised through a confederation of 12 city states (i.e. normally defined as *Decadopoli*) linked one to each other by the same economic, religious, and military interests (Leighton, 2013). Etruscan culture has also been widely documented during the nineteenth and twentieth centuries, thanks to the discovery of numerous *necropolis* with their funerary equipment, being evidence of the degree of their civilization (Steingräber, 2016). In addition, Etruscans are also extremely famous for their metallurgical skills, their ability in gold processing, their aptitude to trade and sail, and having contacts with the most important civilization of the Mediterranean Area (Camporeale, 2016). With the beginning of the third century BC, their civilization started to be absorbed by Romans, and it is worth mentioning that three of the first kings of Rome were Etruscan (Balassone et al., 2018; Camporeale, 1969; Cristofani, 2000; Cristofani & Martelli, 1983; Nestler & Formigli, 2013).

Although much information has been collected regarding the cult of death, very little is known about the world of the living. Several scholars have addressed Etruscan ceramic production technology and provenance (Bruni, 2012; Bruni, Bagnasco Gianni, & Ciarati, 2001; Ciarati, Bruni, & Fermo, 2001; Fermo, Cariati, Ballabio, Consonni, & Bagnasco Gianni, 2004; Ganio, MacLennan, Svoboda, Lyons, & Trentelman, 2021; Gliozzo et al., 2011; Gliozzo, Kirkman, Pantos, & Turbanti, 2004; Longoni et al., 2023; Maritan, 2004; Nodari, Maritan, Mazzoli, & Russo, 2004; Saviano, Drago, Felli, & Violo, 2002), or the effects of local natural resource exploitation to the surrounding environment and people health in the past (Harrison, Cattani, & Turfa, 2010; Magny et al., 2007; Sadori, Mercuri, & Mariotti Lippi, 2010). Regarding Etruscan architecture, available information is scarce (Edlund-Berry, 2011; Miller, 2015; Roos & Wikander, 1986), and only on architectural terracotta a great deal of attention has been directed toward the stylistic and iconographical study of ancient roofs (Lulof, 2014; Meyers, Jackson, & Galloway, 2010; Winter, 2002). Even less data are available regarding the exploitation of local natural resources for construction purposes such as wood, roof tiles, bricks, or earthen-based materials (Amicone, Croce, Castellano, & Vezzoli, 2020; Ammerman et al., 2008; Ceccarelli, Moletti, Bellotto, Dotelli, & Stoddart, 2020; Coradeschi et al., 2021; Weaver, Meyers, Mertzman, Sternberg, & Didaleusky, 2013; Winter, Iliopoulos, & Ammerman, 2009).

Considering the rarity of archaeological sciences studies on architectural construction material from the Etruscan period, several bricks and roof tiles recovered at the *Domus dei Dolia* (*Vetulonia*, Italy) were considered to develop an interdisciplinary study. These materials always had less attention from archaeological science specialists compared to the most famous pottery wares, for example. In any case, the massive production and utilization of construction ceramics in civil architecture can surely be useful/utilized to evaluate the economic organization behind their production, the exploitation of locally available natural resources, and the technology of production. So, by studying these materials, it would be possible to increase our knowledge of Etruscan civil architecture and, widely, the Etruscan world of the living, which is still nowadays largely unknown.

The *Domus dei Dolia* was discovered in 2009, and it is located in the ancient town of *Vetulonia* (*Castiglione della Pescaia* Town Hall, Southern Tuscany, Italy). The study of the archaeological evidence made possible the documentation of an almost entire Etruscan house, probably occupied between the third and the first century BC (Coradeschi et al., 2021; Rafanelli et al., 2018), in the last centuries of its Etruscan History. Among the different materials collected, we can mention different ceramic wares, mortars, wall painting fragments, votive bronze statues, coins, nails, numerous charred woods, wattle and daub earthen construction materials, in addition to several bricks and roof tiles.

The utilization of bricks has been widely attested in the Etruscan world as an important architectural component (Pizzirani, 2019). They were normally unfired, and dimensions and shape could be adapted depending on architectural needs (i.e. width of the wall or foundation). Non-decorated roof tiles are generally abundant in most sites, and differently from bricks, they were generally fired (Bonetto, 2019; Ceccarelli et al., 2020). Two different roof-tile shapes were normally employed in Etruscan architecture (Meyers et al., 2010). They could be planar (pan roof tiles – *tegulae*) or semi-circular (cover roof tiles – *imbrices*), and these architectural elements represent the basic units of a typical terracotta pitched roof in Etruria. The production was quite standardized (Meyers et al., 2010). A pan roof tile was generally rectangular in shape, and it could be long, up to 65/70 cm, and up to 50 cm wide, with raised side borders on the longest sides. Normally positioned

one close to another, the bottom part of each *tegulae* overlapped the top of the *tegulae* below it, starting from the higher part of the roof to the lower sides. Each curved *imbrices* covers the joints formed between the side ridges of adjacent *tegulae*, and they were also partially superimposed on the smaller side. Using this system, the water could easily flow down the roof, protecting the structure of the house from water infiltration.

The objectives of the study presented in this article are as follows:

1. To evaluate/understand whether the construction materials were locally produced in the town or imported.
2. To evaluate if different raw materials were employed to produce bricks and roof tiles.
3. To understand the technology employed in the production of bricks and roof tiles.
4. To understand the reasoning behind exploiting different raw materials (if confirmed).
5. To evaluate the production organization of construction materials and to get information regarding the local economy.

2 Archaeological Setting

2.1 The Ancient City of Vetulonia and the Identification of the Domus dei Dolia

The city of *Vetulonia* is in central Italy, in the western side of the Italian peninsula in Southern Tuscany (Figure 1). During ancient times, the city overlooked a big navigable lagoon to the west (Colombi, 2018) and also controlled a vast territory to the north, including the so-called area of the *Colline Metallifere*, an important Italian mining district particularly abundant in ore natural resources (Bazzoni, Betti, Casini, Costantini, & Pagani, 2015). The most ancient Etruscan archaeological evidence goes back to the ninth–eleventh century BC, but it was between the eighth and the sixth century that *Vetulonia* gained importance, and it became one of the few important Etruscan city states that survived to Rome expansion until the second century BC. Nevertheless, during the first century BC, the city was involved in the Roman civil war, leading to its inexorable decline and

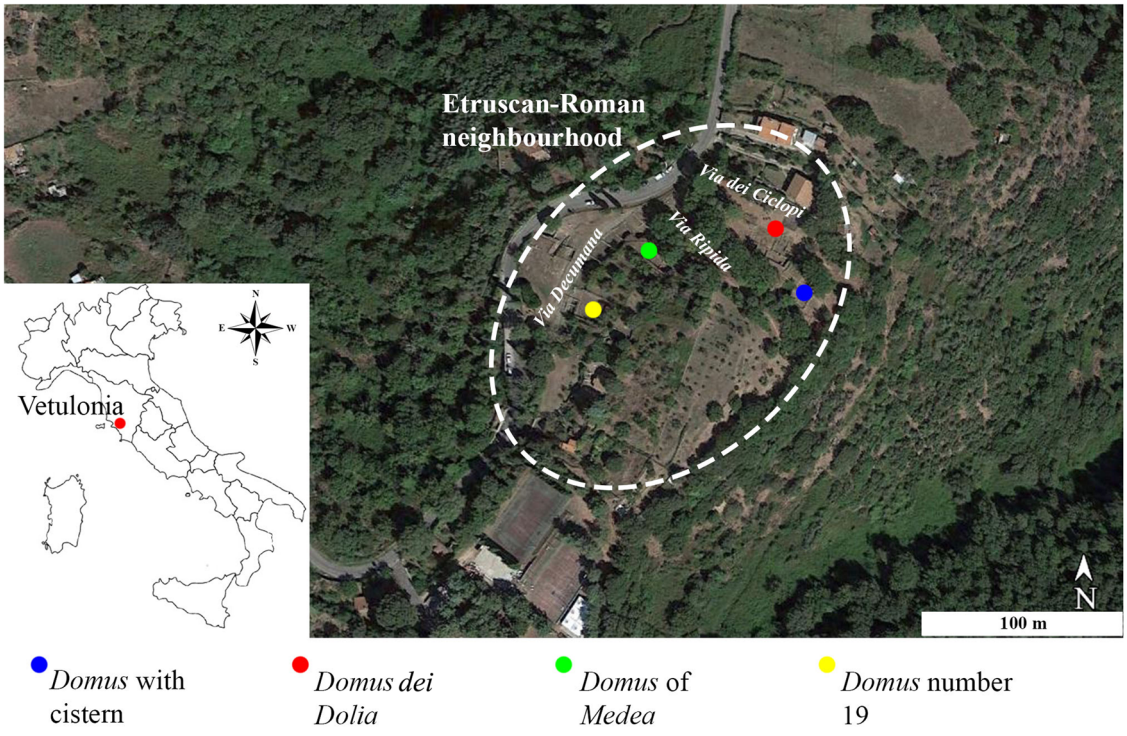

Figure 1: Identification of the Domus dei Dolia within the Etruscan-Roman neighbourhood of Poggiarello Renzetti, Vetulonia, Italy.

destruction (Gregori, 1991; Semplici, 2015). The most ancient archaeological excavation at *Vetulonia* was carried out by *Isidoro Falchi* during the late nineteenth century, discovering the funerary area of the city (i.e. Villanovia phase of the Etruscan Culture, ninth–eighth century BC) in addition to the majestic *tumulus* tombs (Etruscan Orientalizing Period, eighth to beginning of the sixth century BC), and the Etrusco-Roman neighbourhood (Hellenistic – Late Republican periods, third–first centuries BC) of the ancient city in the area of *Poggiarello Renzetti* (Cygeilman, 2002).

Afterwards, since the middle of the twentieth century, new excavations were carried out by different scholars, bringing to light more evidence of the ancient Etruscan city of *Vetulonia* included in the Hellenistic (i.e. fourth–third centuries BC) and Late Republican (i.e. second–first centuries BC) periods (Cygielman, 2015; Rafanelli, 2015; Talocchini, 1981; da Vela, 2015). Just in 2009, in the Etrusco-Roman district discovered by Isidoro Falchi at *Poggiarello Renzetti*, the *Domus dei Dolia* was discovered (Agricoli, Rafanelli, & Carnevali, 2016).

The *Domus* is close to other residential Etruscan houses of the Hellenistic period such as the *Domus* n. 19, the *Domus* of *Medea*, and another *Domus* characterized by the presence of a vast atrium with *impluvium* and a large cistern (Figure 1). Consequently, the Hellenistic residential area of *Poggiarello Renzetti* represents the most important archaeological evidence of ancient *Vetulonia*, representing a period of prosperity and economic renaissance.

The results of the archaeological excavation evidenced that the *Domus* was destroyed by a fire, which probably also destroyed the whole neighbourhood (Cygeilman, 2016) during the Roman civil war of the first century BC. Besides, the preliminary study of pottery (i.e. black painted ware and Greek-Italic amphorae) supports this hypothesis, suggesting a chronological occupation of the house in a timeframe comprised between the third and the first century BC (Grassigli & Rafanelli, 2019; Rafanelli & Spiganti, 2019).

From the architectural point of view, the uncovered reality represents an important discovery in the field of Etruscan archaeology, as the archaeological structures are quite intact (Figure 2), and well-preserved dwellings with a high rise (i.e. 1.60 m high and 0.6 m thick) are still in place. Based on field observation, three different

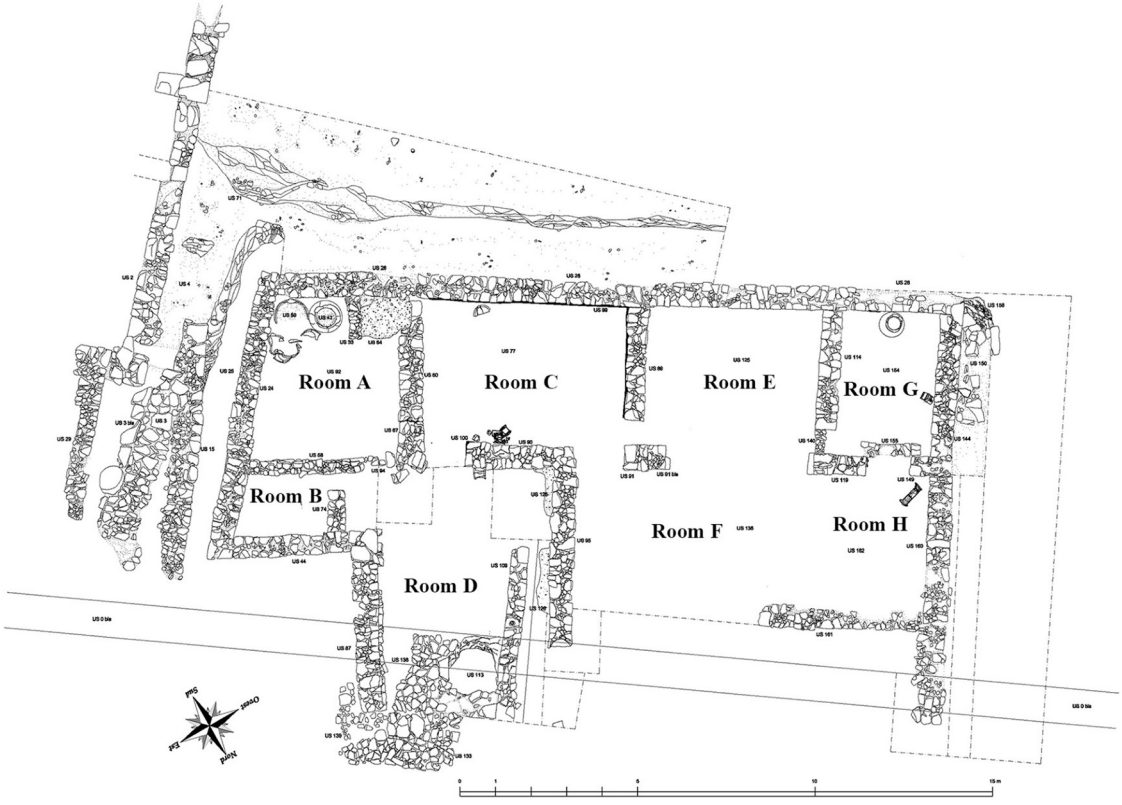

Figure 2: Planimetry of the Domus dei Dolia, and the divisions brought to light between 2009 and 2015.

construction phases have been proposed by archaeologists and, until now (the excavation is still on-going), 12 different divisions of the *Domus* with a different function have been documented. The complete description of the *Domus* can be found elsewhere (Coradeschi et al., 2021; Grassigli & Rafanelli, 2019; Rafanelli & Spiganti, 2019).

Different construction materials were employed to build the *Domus dei Dolia*. Perimetral and dividing walls were mostly constructed using locally available sandstone. Nevertheless, walls could also be constructed

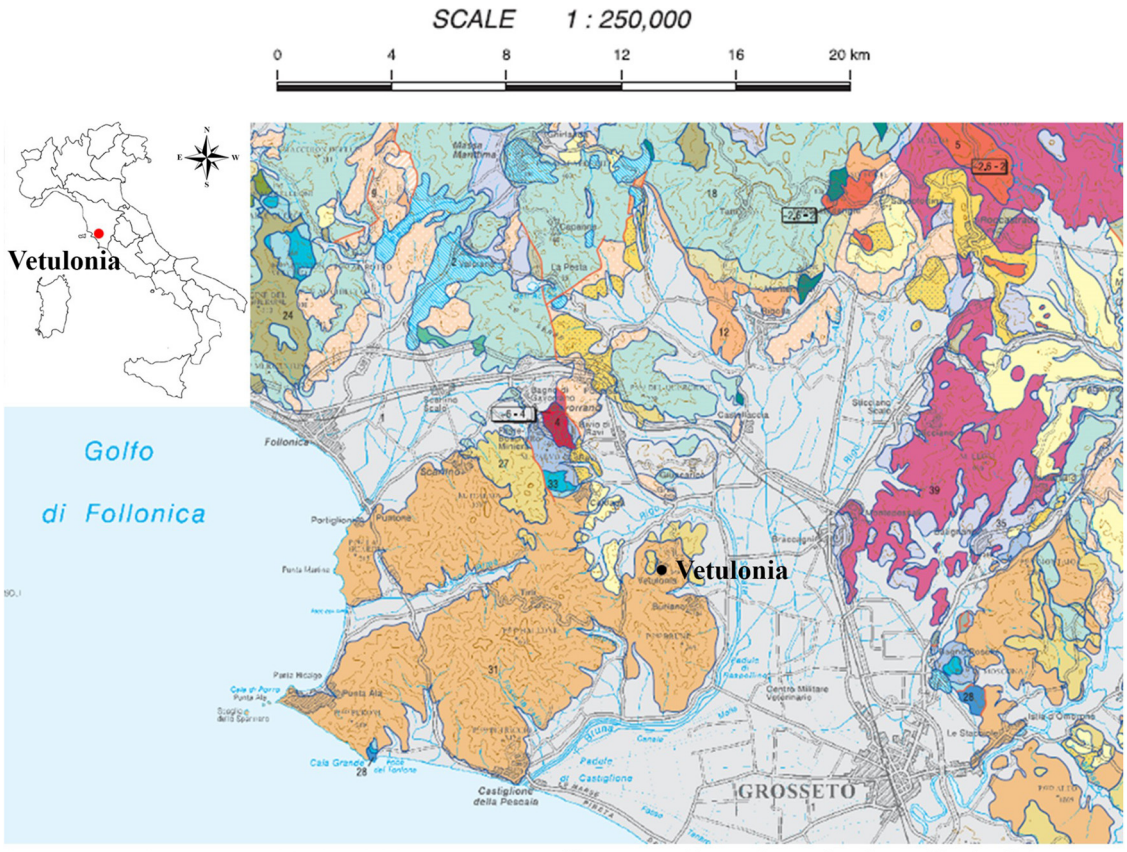

Figure 3: Geological map of the area of Vetulonia where the archaeological site has been discovered. The geological map has been adapted after Carmignani et al. (2013).

using stones (i.e. lower part of the wall) plus bricks or wattle and daub (i.e. higher part of the wall). These technological options have been widely attested in the Etruscan world (Amicone et al., 2020; Ceccarelli et al., 2020; Miller, 2015; Pizzirani, 2019), but they were prohibited and substituted by fired bricks in Roman territories after the first century BC (Spiganti, Trippetti, Spiganti, & Zoccoli, 2016). Wood was utilized for the construction of the room's framing elements, for the doors, and may be for the internal support of wattle and daub (Coradeschi et al., 2021). Finally, roof tiles were used in the roof.

2.2 Geological Setting of the Area

The ancient city of Vetulonia is located on the western side of the Italian Peninsula, in the southern portion of the Tuscany region, roughly 15 km from the seacoast. It is positioned at an altitude of 320 m above sea level with the following coordinates: 42°51′34″N to 10°58′16″E. The geology of the area (Carmignani, Conti, Cornamusini, & Pirro, 2013) is the result of the collision between the African (i.e. Apulia microplate) and European (i.e. Briançonnais microplate) plates during the Tertiary. This event led to the rise of the Northern Apennines (Conti, Cornamusini, & Carmignani, 2020), and in Tuscany, it is possible to observe a complete nappe stack of it, being most geological unit completely exposed. In the area of interest (i.e. Tuscany southwest, Figure 3) the following units can be found: the metamorphic succession of the Tuscan domain, non-metamorphic succession of the Tuscan domain, the Sub-Ligurian domain, the Ligurian domains (i.e. internal and external), in addition to Neogene to Quaternary sedimentary successions. Of all these units derived by the Apulia microplate and the Thetys ocean realm (i.e. Ligurian domains), while the Sub-Ligurian domain represents a transitional domain between the oceanic and the Apulia continental crust. Neogene and quaternary intrusive and effusive acid/felsic volcanic rocks are also present close to the site.

Table 1: Archaeological samples included in this study, including typology, division of the Domus where the sample has been collected, year of recovery, and some sample characteristics

Sample ref.	Roof tile typology	Room/function	Archaeological campaign	Paste colour
VSC1	Pan – *Tegulae*	G/storage room	2015	Buffy
VSC2	Pan – *Tegulae*	H/semi open room with portico	2015	Buffy
VSC3	Pan – *Tegulae*	G/storage room	2015	Red
VSC4	Cover – *imbrices*	G/storage room	2015	Red
VSC5	Cover – *imbrices*	G/storage room	2015	Red-brown
VSC6	Pan – *Tegulae*	H/semi open room with portico	2015	Buffy
VSC7	Pan – *Tegulae*	H/semi open room with portico	2015	Red
VSC8	Pan – *Tegulae*	H/semi open room with portico	2015	Buffy
VSC9	Pan – *Tegulae*	E/tablinum	2013	Red
VSC10	Cover – *imbrices*	H/semi open room with portico	2015	Red
VSC11	Cover – *imbrices*	H/semi open room with portico	2015	Red
VSC12	Cover – *imbrices*	H/semi open room with portico	2015	Red
VSC13	Cover – *imbrices*	H/semi open room with portico	2015	Red
VSC14	Pan – *Tegulae*	E/tablinum	2013	Red
VSC15	Pan – *Tegulae*	E/tablinum	2013	Brown
VSC16	Pan – *Tegulae*	E/tablinum	2013	Buffy
VSC17	Cover – *imbrices*	E/tablinum	2013	Red
VSC18	Cover – *imbrices*	A/storage room	2010	Red-brown
VSC19	Pan – *Tegulae*	A/storage room	2010	Buffy
VSC20	Pan – *Tegulae*	A/storage room	2010	Buffy
VSC21	Pan – *Tegulae*	C/triclinium	2011	Buffy
VSC22	Pan – *Tegulae*	C/triclinium	2011	Red-brown
VSC23	Brick	B/product processing area	2009	Red
VSC24	Brick	B/product processing area	2009	Red

3 Materials and Methods

3.1 Materials

The archaeological excavation of the *Domus dei Dolia* began in 2009 (it is still on-going), and the construction materials included in this study (Table 1) were recovered between 2009 and 2015. During this period, only the southern section of the *Domus* was excavated. Bricks were recovered inside division B, and only some of them were clearly visible during the excavation. In addition, bricks were not fired during the Etruscan period, so humidity, burial conditions, and rain affected their conservation and recovery. Nevertheless, in our case, the *Domus* was destroyed by a fire, and bricks were consequently partially fired (Spiganti et al., 2016), helping the preservation and recovery of some of them. Archaeological data indicated that they were utilized to complete the construction of a dividing wall made up of sandstones that separated division A from division B (Figure 4a and b). The preliminary macroscopic observation of the bricks suggested that the same raw material was probably exploited to produce them, and two samples from two different bricks were selected for analysis. The dimension of bricks could vary depending on preservation, and the registered dimensions were as follows: 20/26 cm long, 16/21 cm wide, and 11/12.5 cm thick (Pozzi, Giancarlo, Beltrame, & Coradeschi, 2016).

Roof tiles were very abundant in all divisions, but few were almost intact. Most roof tiles were extremely fractured because of the roof's collapse (Figure 4b and c). The best-preserved planar roof tile was 71.5 cm long, 52 cm wide, and 3.5 cm thick. The raised side border was 2–3 cm wide, the internal height was 4.3 cm, and the external height was 7.6 cm. In the case of semi-circular roof tiles, just partial fragments were recovered, and they were a maximum of 19.8 cm long and 17.7 cm wide, and the chord was 10 cm maximum (Pozzi et al., 2016). Unlike bricks, planar and semi-circular roof tiles differed in terms of paste colour, suggesting that more than one raw material was probably exploited in their production. In total, 14 pan and nine (9) cover roof tiles were selected from different divisions of the *Domus*, being representative of the different pastes observed during sampling.

Figure 4: (a) Room B, bricks and roof tiles can be observed lying on the top part of the archaeological deposit, (b) bricks from room B, (c) room C, a picture representing many roof tiles completely fragmented on the archaeological deposits with traces of burning.

3.2 Methods

Samples were analysed using optical microscopy (OM), X-ray diffraction (XRD), and X-ray fluorescence (XRF). Principal component analysis (PCA) was used to evaluate XRF results.

3.2.1 OM

OM analysis was performed for all samples. To describe this section, minerals, rocks, and rock fragments were identified in all cases. Ceramic paste, porosity, and temper characteristics were described following the guidelines of Quinn (2013). Temper grain size was described using the Wentworth (1922) classification scale, while grain size distribution and temper abundance were evaluated by 2D image analysis using ImageJ software (Beltrame et al., 2020; Sitzia, Beltrame, & Mirão, 2022). A transmitted light petrographic microscope, model Leica DM-2500-P, equipped with an acquisition camera model Leica MC-170-HD was used for the ceramic thin section analysis. The HRX-01 HIROX microscope, equipped with a 5 MP sensor and HR-5000E lens at 0° inclination, was used to acquire high-resolution images of samples at 140× magnifications.

3.2.2 XRD

XRD analyses were developed on powdered samples. The equipment utilized was a Bruker AXS D8 Discover with the Da Vinci design, using a Cu Kα source and operating at 40 kV and 40 mA. Analyses were performed in the 3 to 75° 2θ, range, with a step of 0.05 2θ, and 1 second/step acquisition time by point. The interpretation of XRD patterns was performed using Diffract-EVA software with a PDF-2 mineralogical database (International Centre for Diffraction Data).

3.2.3 XRF and PCA

XRF was applied in all samples for the quantification of major oxides (SiO_2, TiO_2, Al_2O_3, Na_2O, K_2O, CaO, MgO, MnO, FeO, and P_2O_5) and some trace elements (Rb, Sr, Y, Zr, Nb, Th, U, and Mn), using an S2 Puma (Bruker) energy-dispersive X-ray spectrometer (Beltrame et al., 2019, 2021). Samples (1.2 g) were fused in a Claisse LeNeo heating chamber with the addition of a flux (Li–Tetraborate, 12 g) to prepare fused beads (ratio sample/flux = 1/10). The software utilised for data acquisition and processing was Spectra Elements 2.0, which reported the final oxide/element concentrations and the instrumental statistical error associated with the measurement. The loss on ignition (LOI) was determined by calcining a 1 g dry sample in a muffle furnace for 1 h at 1,100°C. PCA was applied to interpret chemical analysis results (Swan & Sandilands, 1995) including LOI. PCA was developed using a correlation matrix, and a principal component (PC) was considered significant when the eigenvalue was higher than 1. The contribution of each variable (i.e. positive or negative loading) to a PC was assessed as follows. Considering that the sum of the squares of all loadings for an individual PC must equal one, we first calculated the loadings assuming all variables contributed equally to that PC. Afterwards, any variable having a higher loading than the calculated value (i.e. medium value) was considered an important contributor to that PC.

4 Results and Discussion

4.1 OM

Five different fabrics were identified after thin section analysis (Table 2, Figure 5).

Table 2: Synthesis of samples subdivision based on fabrics

Sample ref.	Roof tile typology	Room/function	Fabric
VSC1	Pan	G/storage room	A
VSC2	Pan	H/semi open room with portico	A
VSC3	Pan	G/storage room	B
VSC4	Cover	G/storage room	B
VSC5	Cover	G/storage room	B
VSC6	Pan	H/semi open room with portico	A
VSC7	Pan	H/semi open room with portico	B
VSC8	Pan	H/semi open room with portico	A
VSC9	Pan	E/tablinum	A
VSC10	Cover	H/semi open room with portico	B
VSC11	Cover	H/semi open room with portico	E
VSC12	Cover	H/semi open room with portico	E
VSC13	Cover	H/semi open room with portico	E
VSC14	Pan	E/tablinum	B
VSC15	Pan	E/tablinum	C
VSC16	Pan	E/tablinum	A
VSC17	Cover	E/tablinum	B
VSC18	Cover	A/storage room	B
VSC19	Pan	A/storage room	A
VSC20	Pan	A/storage room	A
VSC21	Pan	C/***triclinium***	A
VSC22	Pan	C/***triclinium***	B
VSC23	Brick	B/product processing area	D
VSC24	Brick	B/product processing area	D

Fabric A (Figure 5a). This fabric includes samples VSC-1/2/6/8/9/16/19/20/21, and they are pan roof tiles. In all cases, the ceramic paste is moderately homogeneous and buffy in colour. The colour of ceramic pastes suggests a high calcium content in the raw clay material employed to produce them. Nevertheless, this consideration will be tested/verified by mineralogical and chemical analysis in Sections 4.2 and 4.3. Porosity is abundant, and it is mainly composed of micro to macrochannels and vughs. Channels are generally weakly oriented to the outer surfaces of the fragments in thin sections. Temper (5 to 10%) is very poorly sorted in all cases, and elongated crystals are more abundant than equant ones. The degree of roundness varies from angular to sub-rounded. Grain size distribution is bimodal. Besides, two distinct grain size fractions could be clearly observed. The smaller fraction is mainly composed of sub-rounded/angular grains of coarse silt, while the coarse fraction is composed of very coarse sand to granule angular grains. From the mineralogical point of view, plagioclase feldspars and pyroxenes were dominant, with lower amounts of quartz, amphiboles (few), potassium-rich feldspar (rarely), and opaque minerals. Gabbroic rock fragments were very common. Shale, siltstone, and sandstone could also be rarely observed, in addition to some fragments of volcanic glass.

Fabric B (Figure 5b). This fabric includes samples VSC-3/4/5/7/10/14/17/18/22, and they are four pans and five cover roof tiles. In all cases, the ceramic paste is slightly homogeneous and red/brown in colour. The colour of ceramic pastes suggests high iron content in the raw clay material employed to produce them. Porosity is not very abundant, and it is mainly composed of micro to meso vesicles and vughs. Temper (5 to 20%) is very poorly sorted in all cases, with a similar concentration of elongated and equant crystals. Roundness varies from angular to sub-rounded. Grain size distribution is mostly bimodal. Besides, two distinct grain size fractions could be clearly observed with a different degree of roundness. The smaller fraction (i.e. more rounded) varies from coarse silt to very fine sand, while the coarse fraction varies from coarse sand to granule. From the mineralogical point of view, quartz, plagioclase, and pyroxene were dominant mineralogical phases compared to muscovite, potassium-rich feldspar, and amphibole minerals. Opaque minerals were also identified in thin sections. Unlike fabric A, shale, siltstone, and sandstone rock fragments were common in all cases, and gabbroic rock fragments were less represented.

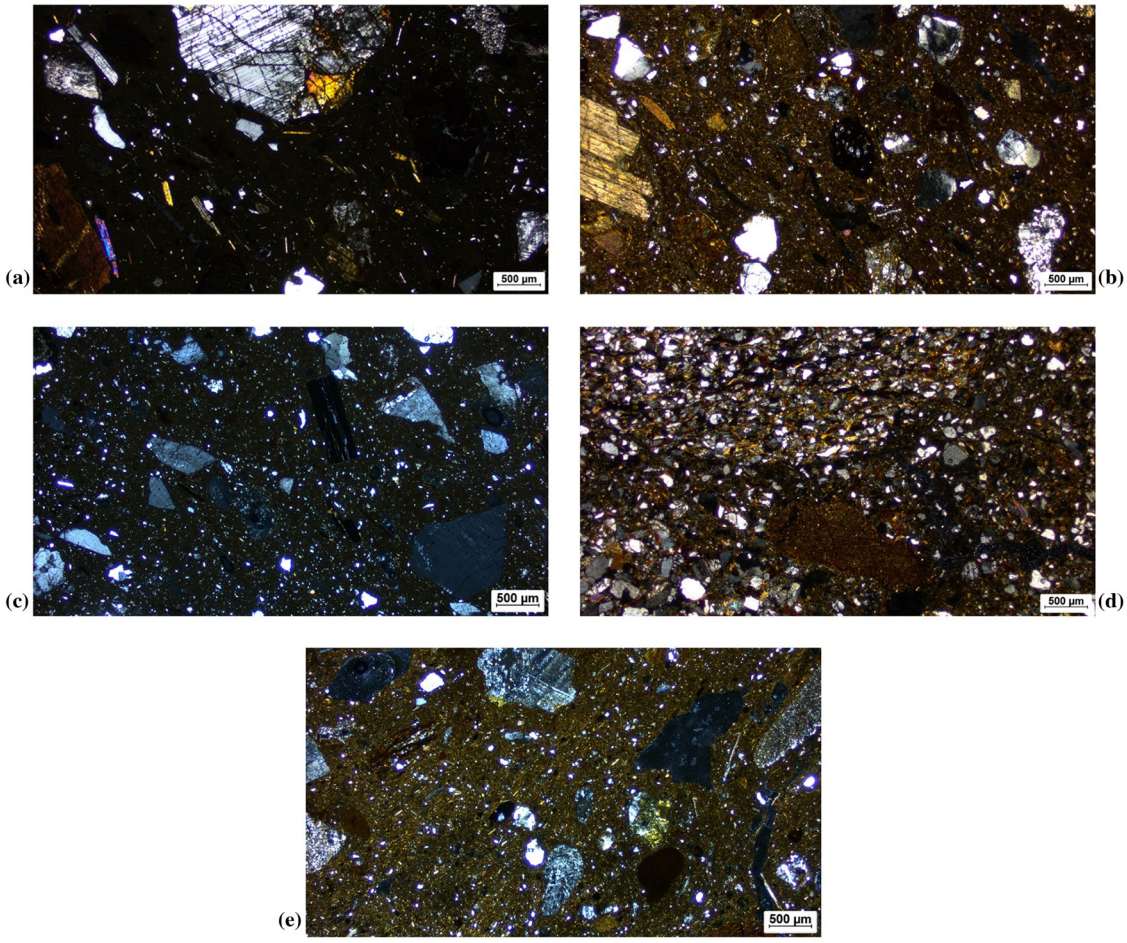

Figure 5: Fabric collected (25× magnification) at crossed polarized light. (a) Fabric A, (b) Fabric B, (c) Fabric C, (d) Fabric D, and (e) Fabric E.

Fabric C (Figure 5c). This fabric includes a sample VSC-15, and it is a pan roof tile. The ceramic paste is moderately homogeneous and brown in colour. Thus, similar to fabric B, the ceramic paste colour suggests high iron content in the raw clay material employed to produce it. Porosity is not very abundant, being mainly composed of micro to meso vesicles and vughs. Temper (20%) is very poorly sorted, predominating equant crystals. Roundness varies from angular to sub-rounded. Grain size distribution is bimodal, and two distinct grain size fractions could be clearly observed. The smaller fraction is composed of sub-rounded/angular grains of coarse silt, while the coarse fraction is composed of angular grains of coarse sand. From the mineralogical point of view, quartz, big crystals potassium-rich feldspar, and biotite mineralogical phases are dominant. Plagioclase feldspars (few), zircon (rare), and opaque minerals could also be observed. Unlike fabrics A and B, granitic rock fragments were common, but a few sandstone fragments were also observed.

Fabric D (Figure 5d). This fabric includes samples VSC-23/24, and they are two bricks. The ceramic paste is moderately homogeneous and red in colour. Thus, similar to fabrics B and C, the ceramic paste colour suggests high iron content in the raw clay material employed to produce them. Porosity is mainly composed of randomly oriented micro to macro vesicles, vughs, and channels. Temper (40–50%) is moderately sorted, with a clear predominance of equant crystals. Roundness varies from sub-rounded to rounded. Grain size distribution is unimodal in all cases, with the predominance of fine sand grains. From the mineralogical point of view, quartz, potassium-rich feldspar, and muscovite are the dominant mineralogical phases, in addition to plagioclase feldspars (few) and opaque minerals. Amongst rock fragments, shale, and sandstone fragments were very abundant.

Fabric E (Figure 5e). This fabric includes samples VSC-11/12/13, and they are semi-circular roof tiles. The ceramic paste is slightly homogeneous and red/brown in colour. Thus, similar to fabrics B, C, and D, the ceramic paste colour suggests high iron content in the raw clay material employed to produce them. Porosity is abundant, slightly alienated to samples margins in thin sections, and it is mainly composed of meso to mega vughs, channels, and planar voids. Temper (5–10%) is very poorly sorted, with a predominance of equant crystals. Roundness varies from angular to sub-rounded. Grain size distribution is bimodal, and two distinct grain size fractions could be clearly observed. The smaller fraction is composed of sub-rounded/angular grains of coarse silt, while the coarse fraction is mainly composed of sub-angular and angular grains of coarse sand. From the mineralogical point of view, quartz is the dominant mineralogical phase, with a lower amount of potassium-rich feldspar, plagioclase feldspars, amphiboles (few), pyroxenes, and opaque minerals. Shale, slate, sandstone, and quartzite were very common, and gabbroic rock fragments (rarely) were rarely identified.

Thin section evaluation evidenced a clear difference in roof tiles and bricks manufacturing technology. In the first case, fabrics A, B, C, and E were largely employed to produce roof tiles. Fabrics A and C were generally utilized to produce pan roof tiles, while fabric E was just utilized to produce cover roof tiles. On the contrary, fabric B could be utilized to produce both pan and cover roof tiles. Our observations suggest that in all cases, the raw material was partially treated, and a bigger inclusion could be added in a second moment. Besides, small and big grains do not generally sediment together, and the presence of sub-rounded inclusion in the smaller grain size fraction also points to a partial treatment of the raw material. Temper amount could change (5–20%) in this category of construction materials. Probably, it was not an important variable or, alternatively, a slightly different amount of tempering material could be added depending on the characteristics of the clayey material employed (loss of volume during drying and firing). This hypothesis would suggest that the clayey raw material employed could be different and heterogeneous for different fabrics.

In the case of bricks (Fabric D), the manufacturing technology employed was completely different. It seems that considering the amount of temper (40–50%), the raw material extracted was not treated at all or, alternatively, just the bigger inclusions were removed from the raw material. Inclusion grain size is quite uniform, and it might support this hypothesis. Maybe this was a specific technological option considering the raw material loss of volume and shrinkage during drying (Ceccarelli et al., 2020). Besides, as already stated in the introductory section, during the Etruscan period, bricks were unfired, and a significant amount of temper was probably needed to preserve the original shape of the brick during drying and to avoid shrinkage.

Regarding the origin of the raw material employed to produce roof tiles and bricks, the exploitation of three different raw materials sources is proposed considering sample characteristics and the geological setting of the area (Figure 3). The first raw material source is represented by fabrics A, B, and E. The colour of ceramic pastes (i.e. buffy, red, and red/brown) suggests that the characteristics of the clayey raw material employed could be slightly different between fabrics and that the sedimentary deposit exploited could be different or heterogeneous. Besides, the ceramic paste of CaO-rich raw materials normally became buffy after firing while, on the contrary, when CaO is not so abundant, it does not. This hypothesis will be verified by XRD and XRF analysis in Sections 4.2 and 4.3, respectively. Regarding inclusions (i.e. minerals and rock fragments), the identification of a similar mineralogical association (i.e. in all cases, mafic minerals such as plagioclase feldspars and pyroxenes were clearly identified in a thin section) suggests/indicates that a raw material with similar mafic inclusions was selected and exploited. The main difference between fabrics A, B, and E resides in the relative abundance of these minerals in sample ceramic pastes. On fabric A, mafic minerals are the dominant mineralogical phases. Conversely, from fabrics B to E, the presence of mafic minerals decreases, while the presence of mineral inclusion such as quartz, muscovite, and potassium-rich feldspars increases. Also, the identification of similar rock fragments points to an analogous interpretation. As in the previous case, mafic (i.e. gabbro rock fragments) and sedimentary (i.e. quartzite, shale, slate, and sandstone) rock fragments were observed in all cases. The presence of mafic rock fragments decreases from fabrics A to E, while the abundance of sedimentary rock fragments increases from fabrics A to E. Considering the geological setting of the area close to the archaeological site, optical microscopy results point to a compatibility with the non-metamorphic succession of the Internal Ligurian Unit (Figure 3) that outcrops in a radius of roughly 4–12 km north/north-east from the archaeological site. They are mainly composed of Jurassic ophiolites (Montanini, Travaglioli, Serri, Dostal, & Ricci, 2006) and their cretaceous sedimentary cover (Carmignani et al., 2013; Conti

et al., 2020; Nirta, Pandelli, Principi, Bertini, & Cipriani, 2005). In particular, the sedimentary cover is made by heterogeneous shales (i.e. dark/grey shale, siliceous limestone, and fine-grained quartz arenite bed), including ophiolitic masses (i.e. olistoliths and sedimentary breccias) of variable dimension. Mafic minerals and rock fragments can only be found within this geological unit, and it is localized in the territory. Consequently, this material was selected and preferred (i.e. considering the number of samples included in these fabrics) to produce roof tiles, and the heterogeneity observed in fabrics A, B, and E reflects the heterogeneity of the selected deposit/s of the same geological formation.

In the case of fabric C, the minerals and rock fragments identified in thin sections (i.e. feldspars, biotite, quartz, zircon, and granite) point to compatibility with the Neogene and Quaternary acid/felsic magmatic outcrops, located at 6–8 km north-east of the archaeological site. In this case, the Gavorrano monzogranites (Musumeci, Mazzarini, Corti, Barsella, & Montanari, 2005) show a similar mineralogical association, suggesting that the alteration products of this geological formation were employed to produce the only fabric C sample. Also, in this case, the outcrop is extremely localized, and a similar mineralogy cannot be found elsewhere close to the archaeological site. Similar outcrops can only be found in the Elba, Giglio, and Montecristo Islands and north of the city of *Piombino* at roughly 50–60 km from the archaeological site (Carmignani et al., 2013; Conti et al., 2020).

Regarding fabric D (i.e. bricks), they are compatible with the outcrops of the non-metamorphic succession of the Tuscan domain, where the archaeological and the town of *Vetulonia* is located (Amendola et al., 2016; Cornamusini, Elter, & Sandrelli, 2002). Besides, the mineralogical association (i.e. quartz, feldspars, and muscovite) and the rock fragments (i.e. shale and sandstone) can be clearly correlated with this geological formation, indicating that bricks were probably produced in close proximity to the archaeological site.

Thus, our observations indicate that roof tiles were possibly not produced in place, and two different sets of raw materials were exploited. These raw materials could be found in a radius of roughly 12 km from the archaeological site. So, they were imported into the city. Considering that the *Domus* is not the only one within the archaeological area of *Vetulonia*, a massive production of roof tiles was required. Consequently, the selection of the geological deposit was likely based on factors such as distance, abundance, accessibility, space to process the raw material, fuel and water availability, and security. Differently, in the case of bricks, they were probably produced very close to the archaeological sites, using a third and completely different raw material. So, for bricks, the raw material was selected according to accessibility and local availability. The technology applied was also different. In the case of roof tiles, there was no distinction in the technology used to produce them, the typology was not an important variable and similar production criteria were employed in all cases. Differently, in the case of bricks, the amount of temper was an important issue, and it had to be high to avoid bricks shrinkage during drying to preserve the original shape. This technological option in brick manufacture has been very common (Nodarou, Frederick, & Hein, 2008) in the Mediterranean area since prehistory.

4.2 XRD

The mineralogical analysis of the samples verified optical microscopy observations, and it added new data to evaluate samples characteristics and the firing technology applied. Moreover, as already stated in previous sections, the *Domus* was destroyed by a fire, and roof tiles and bricks were exposed to a high temperature. Roof tiles were generally fired (Ceccarelli et al., 2020), but bricks were not (Pizzirani, 2019). So, it can be possible to understand to which extent the “destruction” event influenced the original mineralogy of the samples. Based on the results obtained, samples were grouped into five different XRD groups (Table 3), which reflect the subdivision proposed in Section 4.1.

XRD group 1. Fabric A samples are included in this group. Quartz, plagioclase feldspar, pyroxene, and akermanite/gehlenite mineralogical phases were always identified. On the contrary, potassium-rich feldspar, hematite, analcime, amphibole, and illite/muscovite mineralogical phases may or may not be present.

XRD group 2. Fabric B samples are included in this group. Quartz, plagioclase feldspar, potassium-rich feldspars, pyroxene, hematite, and illite/muscovite mineralogical phases were identified in all cases. On the contrary, calcite, and amphibole mineralogical phases may or may not be observed.

XRD group 3. Fabric C samples are included in this group. Quartz, plagioclase feldspars, potassium-rich feldspars, hematite, biotite, and illite/muscovite minerals were identified.

XRD group 4. Fabric D samples are included in this group. Quartz, plagioclase feldspar, potassium-rich feldspars, and illite/muscovite mineralogical phases were identified in all samples. Smectite and chlorite clay minerals were also identified.

XRD group 5. Fabric E samples are included in this group. Quartz, plagioclase feldspar, potassium-rich feldspars, pyroxene, and illite/muscovite mineralogical phases were identified in all cases, while hematite, calcite, and amphibole may or may not be observed.

As observed during optical microscopy analysis, XRD groups 1, 2, and 5 show a slightly different mineralogy. In XRD group 1, plagioclase feldspars and pyroxenes were observed in thin sections, but akermanite/gehlenite (i.e. sorosilicate) minerals were not. Considering ceramic pastes colour (i.e. buffy), the identification of sorosilicate minerals on XRD patterns strongly suggests that plagioclase feldspars (i.e. tectosilicate) and pyroxenes (i.e. inosilicates) also formed during burning within the ceramic paste. Besides, when the carbonate component of the original raw material is significant, high-temperature calcium/magnesium-rich mineralogical phases nucleate at 800°C (Beltrame et al., 2021; Heimann & Maggetti, 2019; Trinidade, Dias, Coroado, & Rocha, 2009). So, plagioclase feldspars and pyroxenes were included in the tempering material, but they also formed in the ceramic paste in addition to akermanite/gehlenite. The same reasoning is not valid in the case of XRD groups 2 and 5, as akermanite/gehlenite was not identified in XRD patterns, and a difference in the carbonate component within the raw material exploited can be assumed.

Table 3: XRD results

SAMPLE	FABRIC	XRD group	Qz	Pl	Kfs	Prx	Amp	Ak-Gh	Cal	Hem	Anl	Bt	Ilt-Ms	Sme	Chl
VSC1	A	1	XXX	XXX		XXX	X	X		X	X				
VSC2	A	1	XX	XXX	X	XXX		X		X			X		
VSC3	B	2	XXXX	XX	X	X	X		X	X			XX		
VSC4	B	2	XXXX	XX	XX	X				X			X		
VSC5	B	2	XXXX	XX	XX	XX				X			TR		
VSC6	A	1	XX	XXX	X	XXX		XX		TR	X				
VSC7	B	2	XXXX	XXX	XX	XXX	X			X			X		
VSC8	A	1	XXX	XXX	XX	XXX		X		TR	XX				
VSC9	A	1	XX	XXX	X	XXX		XX			XX		TR		
VSC10	B	2	XXXX	X	X	X				X			X		
VSC11	E	5	XXXX	X	X	VS	TR			X			XX		
VSC12	E	5	XXXX	X	X	TR	TR		TR	X			X		
VSC13	E	5	XXXX	X	X	TR				X			X		
VSC14	B	2	XXXX	X	XXX	XX	X			X			X		
VSC15	C	3	XXXX	X	XXX					X		XX	TR		
VSC16	A	1	XXX	XXX	VS	XXXX		TR			XX				
VSC17	B	2	XXXX	XX	X	XX	TR			X			X		
VSC18	B	2	XXXX	XX	X	XX				X			X		
VSC19	A	1	XXX	XXX	XX	XXX		X		X	X		X		
VSC20	A	1	XX	XXX	XX	XXX		TR		X			X		
VSC21	A	1	XXX	XXX	X	XXX		X		X	X				
VSC22	B	2	XXXX	XX	XX	XX				X			X		
VSC23	D	4	XXXX	XX	X								XX	X	X
VSC24	D	4	XXXX	XX	X								XX	TR	TR

Qz, quartz; Pl, plagioclase; Kfs, potassium-rich feldspar; Amp, amphibole; Ak-Gh, akermanite-gehlenite; Cal, calcite; Hem, hematite; Anl, analcime; Bt, biotite; Ilt/Ms, illite-muscovite; Sme, smectite; Chl, chlorite; XXXX, very abundant; XXX, abundant; XX, moderate; X, not abundant; TR, traces.

Moreover, considering the same XRD groups, the semi-quantification of quartz, plagioclase feldspar, and pyroxene mineralogical phases clearly change. Quartz abundance increases in XRD groups 2 and 5, while the plagioclase and pyroxene representativity decrease accordingly. These results support the observation developed in the case of XRD group 1, and the interpretation proposed in the optical microscopy section. These observations indicate that the original raw materials employed to produce XRD groups 1, 2, and 5 contained similar mineralogical species (i.e. as inclusion), but on the clayey fraction, the carbonate component could vary. Consequently, XRD patterns reflect the heterogeneity of the original geological formation exploited in their production.

For XRD groups 3 and 4, results corroborate optical microscopy observation.

Regarding firing technology, bricks and roof tile are two different classes of construction materials, and they were produced using a different technology (Bonetto, 2019; Ceccarelli et al., 2020; Pizzirani, 2019). So, different considerations can be made after evaluating XRD results to determine sample's thermal history. Besides, specific mineralogical phases might disappear or nucleate when a clayey raw material is fired. Phyllosilicates and carbonate disappear during firing depending on the maximum firing temperature attained. Illite/muscovite disappear above 950/1,000°C, smectites at 500°C, while chlorite dehydroxylation occurs around 650°C (Beltrame et al., 2020; Maritan, Nodari, Mazzoli, Milano, & Russo, 2006; Trinidade et al., 2009). Between 700 and 800°C, CO_2 is removed from carbonates, and free lime can combine with melted phyllosilicates in the formation of new calcium-rich mineralogical phases (Fabbri, Gualtieri, & Shoval, 2014; Trinidade et al., 2009), including plagioclase feldspars, pyroxenes, and akermanite/gehlenite. This reaction starts at 800°C (Heimann & Maggetti, 2014, 2019; Noll & Heimann, 2016; Trinidade et al., 2009), and it can continue until a higher temperature (i.e. more than 1,000°C). Hematite nucleates at 750°C (Beltrame et al., 2020).

Thus, the identification of clay minerals on bricks (i.e. XRD group 4) indicates that the fire that destroyed the *Domus* was not sufficiently strong for the clay minerals to collapse and disappear from XRD patterns. Besides, bricks were generally unfired, and the identification of clay minerals points to this interpretation. In the case of roof tiles, considering XRD results, the fire did not influence the original mineralogy because the fire temperature was too low. Consequently, the firing technology applied can be established in the case of roof tiles. Regarding XRD group 1, the firing temperature was higher than 800°C and up to 1,000°C, considering that illite/muscovite was not detected in two different samples. Differently, XRD groups 2, 3, and 5 samples were probably fired between 750 and 950°C. Besides, hematite and illite/muscovite were always detected in the analysed samples.

4.3 XRF and PCA

The chemical analysis result table is presented in a separate annexed file. The statistical treatment of sample's chemical composition by PCA extracted five different PCs, and they describe 87.43% of the total variance (Table 4). The first two PCs were the most significant, representing 58.57% of the total variance.

PCs 1 and 2 have different loadings (Table 5). In the case of PC1, the most important were represented by K_2O, TiO_2, Rb, Y, and Zr (i.e. positive), and Na_2O, CaO, MgO, and Sr (i.e. negative). They describe the abundance of these oxides/elements inside the raw material exploited. K_2O and Rb can be hosted both by tectosilicates (i.e.

Table 4: Descriptive table with eigenvalues and percentage of variance of the extracted PCs

PC	Eigenvalue	Percentage of variance (%)	Cumulative (%)
1	7.42	41.24	41.24
2	3.12	17.33	58.57
3	2.48	13.80	72.36
4	1.57	8.74	81.10
5	1.14	6.33	87.43

feldspars) and by phyllosilicates (i.e. illite/muscovite, biotite). They were both identified during optical microscopy (as lithoclasts or individual minerals) and XRD analysis. Titanium oxide, yttrium, and zircon chemical elements are normally hosted by different accessory minerals. Amongst them, oxides (i.e. ilmenite, rutile, anatase) or nesosilicates (i.e. zircon) can be mentioned. These oxides/elements can be present in the finer grain size fraction of a sediment, sedimentary, and felsic/acid rocks. CaO, MgO, and Sr might represent samples carbonate component, but these oxides (i.e. including Na_2O)/chemical elements can also be hosted by some mafic minerals, such as tectosilicates and inosilicates (i.e. plagioclase feldspars, pyroxenes, and amphiboles). So, PC1 describes the variation of the sedimentary/felsic vs the carbonate/mafic components inside the analysed samples, and these characteristics are widely discussed in Sections 4.1 and 4.2.

Regarding PC2, significant positive loading has been observed in the case of Al_2O_3, P_2O_5, Fe_2O_3, U, and LOI, contrasted by a negative loading of SiO_2 (Table 4). While the variability of uranium and phosphorous is not clear, Al_2O_3, Fe_2O_3, and LOI give important indications. Aluminium and iron oxides are important components in phyllosilicates, while LOI represents hydrous minerals (i.e. mainly phyllosilicates and amphiboles). SiO_2 (i.e. silica) can be included inside different mineralogical phases, and quartz (i.e. tectosilicates) is probably the most significant in this case. So, PC2 describes the amount of hydrous minerals (i.e. mainly phyllosilicates) compared to the amount of quartz (i.e. tectosilicates) inside the analysed samples. Thus, PC2 describes the clay to temper ratio. Nevertheless, in our case, the clay-to-temper ratio was not established, and only an estimation of temper by image analysis was included in the optical microscopy section.

Thus, the biplot (Figure 6) clearly summarizes sample subdivision based on their characteristics, and by combining OM and XRD results, the following observation can be made on fabrics:

1. The chemical composition of fabrics A, B, and E (i.e. XRD groups 1, 2, and 5) samples is explained by the variation of the carbonate component inside the ceramic paste, the variation of mafic and sedimentary minerals/rock fragments, and the clay-to-temper ratio.
2. Fabric A (i.e. XRD group 1) samples are rather uniform in chemical composition, and the carbonate/mafic component was extremely important in this case.
3. Fabric B (i.e. XRD group 2) samples show stronger variability along the PC2 axe. Besides, temper evaluation by 2D image analysis also shows the biggest temper concentration range (i.e. 5–20%). Moreover, the importance of the carbonate/mafic components decreases when compared to fabric A samples.
4. Fabric E (i.e. XRD group 5) samples are rather uniform in chemical composition, and the abundance of clay, sedimentary minerals, and rock fragments were important components in this case.

Table 5: Loading values of PC1 and PC2 for each oxide, chemical element, and LOI. Bold values represent significant PC1 and PC2 loadings

Variables	Loadings of PC1	Loadings of PC2
N_2O	**−0.25**	−0.18
MgO	**−0.32**	0.14
Al_2O_3	0.02	**0.4**
SiO_2	0.2	**−0.44**
P_2O_5	0.16	**0.31**
K_2O	**0.3**	−0.14
CaO	**−0.3**	0.1
TiO_2	**0.29**	0.13
Fe_2O_3	0.22	**0.36**
Rb	**0.29**	−0.08
Sr	**−0.27**	0.1
Y	**0.31**	0.01
Zr	**0.29**	−0.17
Nb	0.23	0.21
Th	0.23	0.17
U	−0.08	**0.28**
Mn	0.01	0.09
LOI	0.05	**0.34**

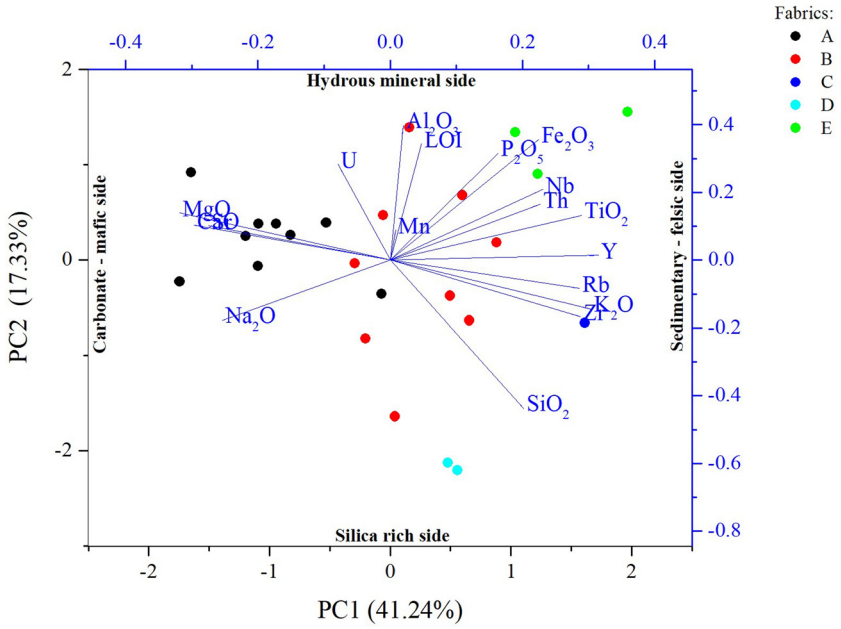

Figure 6: Bi-plot of PC1 and PC2. Blue axes represent PC1 and PC2 loadings for all variables presented in Table 4, while black axes represent sample scores for PC1 and PC2.

5. The chemical composition of fabric C (i.e. XRD group 3) samples is explained by the abundance of felsic mineral and rock fragments. Besides, quartz, biotite, and potassium-rich feldspars were important mineralogical phases, as evidenced by optical microscopy and XRD results. Also, the zircon mineral was an important component of the raw material exploited.
6. The chemical composition of fabric D (i.e. XRD group 4) samples is explained by the abundance of quartz and sedimentary rock fragments and minerals. As evidenced during optical microscopy observation, this fabric was extremely abundant in temper.

5 Conclusions

The archaeological and archaeometrical study evidenced that construction materials were presumably manufactured close to the archaeological site. Roof tiles were most probably produced within 4–12 km from the *Domus*, and the exploitation of two different raw material sources has been proposed. In both cases, the raw material was partially treated, temper could be added in a second moment, and they were fired. Considering that the *Domus dei Dolia* was not the only civil construction in the ancient Etruscan city of *Vetulonia*, it is supposed that a big production of roof tiles was needed for the ancient city. In any case, production sites (i.e. kilns) were never documented close to the archaeological area, but our study suggests that productive areas could be located close to the geological formations exploited. Seemingly, the location could be selected considering the distance from the raw material source, raw material abundance, accessibility, space to process the raw material, water, fuel to fire roof tiles, and security (i.e. in the case of a fire). Maybe, all (or some) of these factors did not favour the utilization of fabric C to produce roof tiles. Conversely, bricks could be produced very close to the archaeological site using specific criteria; the amount of temper was an important variable, and they were not fired. So, security was not a problem, and the selection of the raw material sources was just based on factors such as availability and accessibility. To conclude, this study added new information regarding the technology employed by the Etruscan of *Vetulonia* in producing roof tiles and bricks and suggested a production organization model.

Abbreviations

VSC	Vetulonia Scavi
PCA	principal component analysis
PC	principal component
Qz	Quartz
Pl	Plagioclase
Kfs	potassium rich feldspar
Amp	amphibole
Ak-Gh	akermanite–gehlenite
Cal	calcite
Hem	hematite
Anl	analcime
Bt	biotite
Ilt/Ms	illite-muscovite
Sme	smectite
Chl	chlorite
XXXX	very abundant
XXX	abundant
XX	moderate
X	not abundant
TR	traces
LOI	loss on ignition

Acknowledgments: The corresponding author wish to acknowledge the Municipality of Castiglione della Pescaia (Italy), the Isidoro Falchi Civic Archaeological Museum (Italy), the HERCULES Laboratory funded by the "Fundação para Ciência e Tecnologia" (project codes: UIDB/04449/2020 and UIDP/04449/2020), and the China-Portugal Joint Laboratory of Cultural Heritage Conservation Science supported by the Belt and Road Initiative – National Key R&D Program of China (2021YFE0200100).

Funding information: This work was partly funded by the Municipality of *Castiglione della Pescaia*, Italy. Laboratory analyses were developed in the framework of the Hercules Laboratory projects funded by the Portuguese "*Fundação para Ciência e Tecnologia*" (project codes: UIDB/04449/2020 and UIDP/04449/2020).

Author contributions: Massimo Beltrame – Ginevra Coradeschi – José Mirão: funding acquisition, methodology, conceptualization, archaeometric analysis, data interpretation, data validation, writing first draft, review, editing. Simona Rafanelli – Costanza Quaratesi: archaeological excavation, archaeological excavation data preparation, archaeological materials collection and description.

Conflict of interest: The authors state no conflict of interest.

Data availability statement: The complete XRF datasets generated during and/or analysed during the current study are available in the form of supplementary material.

References

Agricoli, G., Rafanelli, S., & Carnevali, S. (2016). *Vetulonia. La Domus dei Dolia*. Arcidosso, Italy: Effigi.

Amendola, U., Perri, F., Critelli, S., Monaco, P., Cirilli, S., Trecci, T., & Rettori, R. (2016). Composition and provenance of the Macigno Formation (Late Oligocene-Early Miocene) in the Trasimeno Lake area (northern Apennines). *Marine and Petroleum Geology*, *69*, 146–167. doi: 10.1016/j.marpetgeo.2015.10.019.

Amicone, S., Croce, E., Castellano, L., & Vezzoli, G. (2020). Building Forcello: Etruscan wattle-and-daub technique in the Po Plain (Bagnolo San Vito, Mantua, northern Italy). *Archaeometry*, *62*(3), 521–537. doi: 10.1111/arcm.12535.

Ammerman, A. J., Iliopoulos, I., Bondioli, F., Filippi, D., Hilditch, J., Manfredini, A., … Winter, N. A. (2008). The clay beds in the Velabrum and the earliest tiles in Rome. *Journal of Roman Archaeology*, *21*, 7–30. doi: 10.1017/S1047759400004359.

Balassone, G., Mercurio, M., Germinario, C., Grifa, C., Villa, I. M., Di Maio, G., … Langella, A. (2018). Multi-analytical characterization and provenance identification of protohistoric metallic artefacts from Picentia-Pontecagnano and the Sarno valley sites, Campania, Italy. *Measurement*, *128*, 104–118. doi: 10.1016/j.measurement.2018.06.019.

Bazzoni, C., Betti, C., Casini, A., Costantini, A., & Pagani, G. (2015). *Minerali: Bellezze della natura nel parco delle Colline Metallifere – Tuscan Mining Geopark*. In A. Costantini & G. Pagani (Eds.), Ospedaletto – Pisa: Pacini Editore Spa.

Beltrame, M., Liberato, M., Mirão, J., Santos, H., Barrulas, P., Branco, F., … Schiavon, N. (2019). Islamic and post Islamic ceramics from the town of Santarém (Portugal): The continuity of ceramic technology in a transforming society. *Journal of Archaeological Science: Reports*, *23*, 910–928. doi: 10.1016/j.jasrep.2018.11.029.

Beltrame, M., Sitzia, F., Arruda, A. M., Barrulas, P., Barata, F. T., & Mirão, J. (2021). The Islamic ceramic of the Santarém Alcaçova: Raw materials, technology, and trade. *Archaeometry*, *63*(6), 1157–1177. doi: 10.1111/arcm.12671.

Beltrame, M., Sitzia, F., Liberato, M., Santos, H., Barata, F. T., Columbu, S., & Mirão, J. (2020). Comparative pottery technology between the Middle Ages and Modern times (Santarém, Portugal). *Archaeological and Anthropological Sciences*, *12*(7), 130. doi: 10.1007/s12520-020-01053-x.

Bonetto, J. (2019). Diffusione ed uso del mattone cotto nell Cisalpina romana tra ellenizazzione e romanizazzione. In J. Bonetto, E. Bukowiecki, & R. Volpe (Eds.), *Alle origini del laterizio romano. Nascita e diffusione del mattone cotto nel Mediterraneo tra IV e I secolo a.C.* Roma: Edizioni Quasar.

Bruni, S. (2012). Le analisi chimiche nello studio dei materiali ceramici. In M. Bonghi Jovino & G. Bagnasco Gianni (Eds.), *Tarquinia. Il Santuario dell'Ara della Regina. I templi Arcaici* (pp. 421–423). Roma: L'Erma di Bretschneider.

Bruni, S., Bagnasco Gianni, G., & Ciarati, F. (2001). Spectroscopic characterization of Etruscan depurata and impasto pottery from the excavation at Pian di Civita in Tarquinia (Italy): A comparison with local clay. In I. C. Druc (Ed.), *Archaeology and clay* (Vol. 942, pp. 27–38). Oxford: Bar Internationa Series.

Camporeale, G. (1969). *I Commerci di Vetulonia in Età Orientalizzante*. Firenze, Italy: Sansone Editore.

Camporeale, G. (2016). The Etruscans and the Mediterranean. In S. Bell & A. A. Carpino (Eds.), *A Companion to the Etruscans* (pp. 67–86). Chichester, West Sussex, UK: Wiley. doi: 10.1002/9781118354933.ch6.

Carmignani, L., Conti, P., Cornamusini, G., & Pirro, A. (2013). Geological map of Tuscany (Italy). *Journal of Maps*, *9*(4), 487–497. doi: 10.1080/17445647.2013.820154.

Ceccarelli, L. (2016). The Romanization of Etruria. In S. Bell & A. A. Carpino (Eds.), *A companion to the Etruscans* (pp. 28–40). Chichester, West Sussex, UK: Wiley. doi: 10.1002/9781118354933.ch3.

Ceccarelli, L., Moletti, C., Bellotto, M., Dotelli, G., & Stoddart, S. (2020). Compositional characterization of Etruscan earthen architecture and ceramic production. *Archaeometry*, *62*(6), 1130–1144. doi: 10.1111/arcm.12582.

Ciarati, F., Bruni, S., & Fermo, P. (2001). Sezione tecnologica. In G. Bonghi Jovino, G. Bagnasco, & S. Businaro (Eds.), *Tarquinia. Scavi sistematici dell'abitato.Campagne 1982–1988. I materiali* (Vol. 2, pp. 525–537). Rome: L'Erma di Bretschneider.

Colombi, C. (2018). Castiglione della Pescaia (Grosseto), Italien. Auf der Suche nach den Häfen der etruskischen Stadt Vetulonia. Die Arbeiten der Jahre 2016 bis 2018. *E-Forschungsberichte*, *2*, 79–85. doi: 10.34780/c1f9-2c9f.

Conti, P., Cornamusini, G., & Carmignani, L. (2020). An outline of the geology of the northern Apennines (Italy), with geological map at 1:250,000 scale. *Italian Journal of Geosciences*, *139*(2), 149–194. doi: 10.3301/IJG.2019.25.

Coradeschi, G., Beltrame, M., Rafanelli, S., Quaratesi, C., Sadori, L., & Barrocas Dias, C. (2021). The wooden roof framing elements, furniture and furnishing of the Etruscan Domus of the Dolia of Vetulonia (Southern Tuscany, Italy). *Heritage*, *4*(3), 1938–1961. doi: 10.3390/heritage4030110.

Cornamusini, G., Elter, F., & Sandrelli, F. (2002). The Corsica-Sardinia Massif as source area for the early Northern Apennines foredeep system: Evidence from debris flows in the "Macigno costiero" (Late Oligocene, Italy). *International Journal of Earth Sciences*, *91*(2), 280–290. doi: 10.1007/s005310100212.

Cristofani, M. (2000). *Gli Etruschi. Una nuova immagine*. Firenze, Italy: Giunti Editore.

Cristofani, M., & Martelli, M. (1983). *L'oro degli Etruschi*. Novara, Italy: De Agostini Editore.

Cygeilman, M. (2002). *Vetulonia Museo Civico Archeologico "Isidoro Falchi" Guida*. Firenze, Italy: Arti Grafiche Nencini.

Cygeilman, M. (2016). La città antica di Vetulonia. Il quartiere di Poggiarello Renzetti. In S. Rafanelli, G. Agricoli, & S. Carnevali (Eds.), *Vetulonia. La Domus dei Dolia: Vol. I* (Archeologia Itinera, pp. 11–14). Arcidosso, Italy: Effigi.

Cygielman, M. (2015). Medea a Vetulonia. In *Il Museo Civico Archeologico Isidoro Falchi di Vetulonia*. Rome: Edizioni Quasar.

Edlund-Berry, I. (2011). Etruscan architecture. In *Classics*. Oxford, UK: Oxford University Press. doi: 10.1093/obo/9780195389661-0121.

Fabbri, B., Gualtieri, S., & Shoval, S. (2014). The presence of calcite in archeological ceramics. *Journal of the European Ceramic Society*, *34*(7), 1899–1911. doi: 10.1016/j.jeurceramsoc.2014.01.007.

Fermo, P., Cariati, F., Ballabio, D., Consonni, V., & Bagnasco Gianni, G. (2004). Classification of ancient Etruscan ceramics using statistical multivariate analysis of data. *Applied Physics A*, *79*(2), 299–307. doi: 10.1007/s00339-004-2520-6.

Ganio, M., MacLennan, D., Svoboda, M., Lyons, C., & Trentelman, K. (2021). Portrait of an Etruscan Athletic Official: A multi-analytical study of a painted terracotta wall panel. *Heritage*, *4*(4), 4596–4608. doi: 10.3390/heritage4040253.

Gliozzo, E., Comini, A., Cherubini, A., Ciacci, A., Moroni, A., & Memmi, I. T. (2011). Ceramic production and metal working at the Trebbio archaeological site (Sansepolcro, Arezzo, Italy). In *Proceedings of the 37th International Symposium on Archaeometry, 13th–16th May 2008, Siena, Italy* (pp. 61–69). Berlin, Heidelberg: Springer Berlin Heidelberg. doi: 10.1007/978-3-642-14678-7_9.

Gliozzo, E., Kirkman, I. W., Pantos, E., & Turbanti, I. M. (2004). Black gloss pottery: Production sites and technology in Northern Etruria, Part II: Gloss technology. *Archaeometry*, *46*(2), 227–246. doi: 10.1111/j.1475-4754.2004.00154.x.

Grassigli, G. L., & Rafanelli, S. (2019). La Domus "Dei Dolia" nel quartiere di Poggiarello Renzetti a Vetulonia (GR). *Bollettino Di Archeologia On-Line*, *X*(1–2), 169–191.

Gregori, D. (1991). Una bottega vetuloniese di buccheri e di impasti orientalizzanti decorati a stampiglia. In F. Paoli & F. Nicosia (Eds.), *Studi e materiali. Scienze dell'antichità in Toscana: Vol. VI* (pp. 64–81). Firenze: Regione Toscana – L'Erma di Bretschneider.

Harrison, A. P., Cattani, I., & Turfa, J. M. (2010). Metallurgy, environmental pollution and the decline of Etruscan civilisation. *Environmental Science and Pollution Research*, *17*(1), 165–180. doi: 10.1007/s11356-009-0141-5.

Heimann, R. B., & Maggetti, M. (2014). *Ancient and historical ceramics. Materials, technology, art and culinary tradition*. Stuttgrat: Schweizerbart Science Pubblisher.

Heimann, R. B., & Maggetti, M. (2019). The struggle between thermodynamics and kinetics: Phase evolution of ancient and historical ceramics. *European Mineralogical Union Notes in Mineralogy*, *20*, 233–281. doi: 10.1180/EMU-notes.20.6.

Leighton, R. (2013). Urbanization in Southern Etruria from the tenth to the sixth century BC: The origin and growth of major centres. In J. MacIntosh Turfa (Ed.), *The Etruscan world* (pp. 134–150). London: Routledge.

Longoni, M., Calore, N., Marzullo, M., Teseo, D., Duranti, V., Bagnasco Gianni, G., & Bruni, S. (2023). Bucchero ware from the Etruscan town of Tarquinia (Italy): A study of the production site and technology through spectroscopic techniques and multivariate data analysis. *Ceramics*, *6*(1), 584–599. doi: 10.3390/ceramics6010035.

Lulof, P. S. (2014). Terracotta architectural sculpture in classical archaeology. *In* Encyclopedia of global archaeology (pp. 7273–7278). New York, NY: Springer New York. doi: 10.1007/978-1-4419-0465-2_1440.

Magny, M., de Beaulieu, J.-L., Drescher-Schneider, R., Vannière, B., Walter-Simonnet, A.-V., Miras, Y., … Leroux, A. (2007). Holocene climate changes in the central Mediterranean as recorded by lake-level fluctuations at Lake Accesa (Tuscany, Italy). *Quaternary Science Reviews*, *26*(13–14), 1736–1758. doi: 10.1016/j.quascirev.2007.04.014.

Maritan, L. (2004). Archaeometric study of Etruscan-Padan type pottery from the Veneto region: Petrographic, mineralogical and geochemical-physical characterisation. *European Journal of Mineralogy*, *16*(2), 297–307. doi: 10.1127/0935-1221/2004/0016-0297.

Maritan, L., Nodari, L., Mazzoli, C., Milano, A., & Russo, U. (2006). Influence of firing conditions on ceramic products: Experimental study on clay rich in organic matter. *Applied Clay Science*, *31*(1–2), 1–15. doi: 10.1016/j.clay.2005.08.007.

Meyers, G. E., Jackson, L. M., & Galloway, J. (2010). The production and usage of non-decorated Etruscan roof-tiles, based on a case study at Poggio Colla. *Journal of Roman Archaeology*, *23*, 303–319. doi: 10.1017/S1047759400002415.

Miller, P. (2015). *Continuity and change in Etruscan domestic architecture: A study of building techniques and materials from 800–500 BC*. (PhD thesis). University of Edinburgh, Edinburgh, UK.

Montanini, A., Travaglioli, M., Serri, G., Dostal, J., & Ricci, C. A. (2006). Petrology of gabbroic to plagiogranitic rocks from southern Tuscany (Italy): Evidence for magmatic differentiation in an ophiolitic sequence. *Ofioliti*, *31*(2), 55–69.

Musumeci, G., Mazzarini, F., Corti, G., Barsella, M., & Montanari, D. (2005). Magma emplacement in a thrust ramp anticline: The Gavorrano Granite (northern Apennines, Italy). *Tectonics*, *24*(6), 1–17. doi: 10.1029/2005TC001801.

Neil, S. (2016). Materializing the Etruscans. In Sinclair Bell & A. A. Carpino (Eds.), *A companion to the Etruscans* (pp. 15–27). Chichester, West Sussex, UK: Wiley. doi: 10.1002/9781118354933.ch2.

Nestler, G., & Formigli, E. (2013). *Granulazione Etrusca. Un'antica arte Orafa*. Poggibonsi, Siena, Italy: Arti Grafiche Nencini.

Nirta, G., Pandelli, E., Principi, G., Bertini, G., & Cipriani, N. (2005). The Ligurian unit of Southern Tuscany. *Bollettino Della Società Geologica Italiana*, *3*, 29–54.

Nodari, L., Maritan, L., Mazzoli, C., & Russo, U. (2004). Sandwich structures in the Etruscan-Padan type pottery. *Applied Clay Science*, *27*(1–2), 119–128. doi: 10.1016/j.clay.2004.03.003.

Nodarou, E., Frederick, C., & Hein, A. (2008). Another (mud)brick in the wall: Scientific analysis of Bronze Age earthen construction materials from East Crete. *Journal of Archaeological Science*, *35*(11), 2997–3015. doi: 10.1016/j.jas.2008.06.014.

Noll, W., & Heimann, R. B. (2016). *Ancient old world pottery. Materials, technology, and decoration*. Stuttgrat, Germany: E. Schweizerbart'Sche Varlagsbuchhandlung Pubblisher.

Pizzirani, C. (2019). Tecniche costruttive nell'edilizia domestica etrusca tra il VI e IV secolo a.C. In J. Bonetto, E. Bukowiecki, & R. Volpe (Eds.), *Alle origini del latterizzio romano. Nascita e diffusione del mattone cotto nel Mediterraneo tra il IV e I secolo a.C.* (pp. 335–344). Roma: Edizioni Quasar.

Pozzi, S., Giancarlo, A., Beltrame, M., & Coradeschi, G. (2016). Catalogo. In S. Rafanelli (Ed.), *Bentornati a Casa. La Domus dei Dolia riapre le porte dopo duemila anni* (pp. 56–71). Monteriggioni, Siena: Ara Edizioni.

Quinn, P. S. (2013). *Ceramic petrography the interpretation of archaeological pottery & related artefacts in thin section*. Summertown, Oxford, UK: Archaeopress.

Rafanelli, S. (2015). Le mura di Vetulonia. In *Il museo Civico Archeologico Isidoro Falchi di Vetulonia* (pp. 20–21). Arcidosso, Italy: Effigi.

Rafanelli, S., Moita, P., Mirão, J., Carvalho, A., Braga, P., Vicente, R., … Coradeschi, G. (2018). Etruscan render mortars from Domus dei Dolia (Vetulonia, Italy). In *Conserving cultural heritage* (pp. 141–143). London, UK: CRC Press, Taylor and Francis group. doi: 10.1201/9781315158648-36.

Rafanelli, S., & Spiganti, S. (2019). La città di Vetulonia in età ellenistica. Nuovi dati sul circuito murario urbano e sulla nuova Domus dei Dolia. In L. Attenni (Ed.), *Le mura poligonali. Atti del Sesto Seminario con una sezione sul Museo Civico di Alatri* (pp. 123–143). Napoli: Valtrend Editore.

Roos, P., & Wikander, O. (1986). Architettura Etrusca nel Viterbese. Ricerche svedesi a San Giovanale e Acquarossa 1956–1986 *(De Luca Editore)*. Roma: De luca editore.

Sadori, L., Mercuri, A. M., & Mariotti Lippi, M. (2010). Reconstructing past cultural landscape and human impact using pollen and plant macroremains. *Plant Biosystems – An International Journal Dealing with All Aspects of Plant Biology*, *144*(4), 940–951. doi: 10.1080/11263504.2010.491982.

Saviano, G., Drago, L., Felli, F., & Violo, M. (2002). Architectural decorations, ceramics and terracotta from Veii (Etruria): A preliminary study. *Periodico Di Mineralogia*, *71*, 203–215.

Semplici, A. (2015). *Il Museo Civico Archeologico Isidoro Falchi di Vetulonia (Effigi)*. Arcidosso, Italy: Effigi.

Sitzia, F., Beltrame, M., & Mirão, J. (2022). The particle-size distribution of concrete and mortar aggregates by image analysis. *Journal of Building Pathology and Rehabilitation*, *7*(74), 1–17. doi: 10.1007/s41024-022-00214-w.

Spiganti, F., Trippetti, S., Spiganti, S., & Zoccoli, C. (2016). Le tecniche edilizie. In G. Agricoli, S. Rafanelli, & S. Carnevali (Eds.), *Vetulonia. La Domus dei Dolia: Vol. I* (Archeologia Itinera, pp. 21–28). Arcidosso, Italy: Effigi.

Steingräber, S. (2016). Rock tombs and the world of the Etruscan Necropoleis. In *A Companion to the Etruscans* (pp. 146–161). Chichester, West Sussex, UK: Wiley. doi: 10.1002/9781118354933.ch11.

Stoddart, S. (2016). Beginnings. In S. Bell & A. A. Carpino (Eds.), *A companion to the Etruscans* (pp. 1–14). Chichester, West Sussex, UK: Wiley. doi: 10.1002/9781118354933.ch1.

Swan, A. R. H., & Sandilands, M. (1995). *Introduction to geological data analysis*. Oxford: Blackwell Science.

Talocchini, A. (1981). Ultimi dati offerti dagli scavi vetuloniensi. *Atti Del XII Convegno Di Studi Etruschi e Italici, 16–20 Giugno 1979* (pp. 100–138). Firenze: Istituto Italiano di Studi Etruschi ed Italici.

Trinidade, M. J., Dias, M. I., Coroado, J., & Rocha, F. (2009). Mineralogical transformations of calcareous rich clays with firing: A comparative study between calcite and dolomite rich clays from Algarve, Portugal. *Applied Clay Science*, *42*(3–4), 345–355. doi: 10.1016/j.clay.2008.02.008.

da Vela, R. (2015). Un database relazionale ed un network di verifica per l'edizione degli scavi di Anna Talocchini a Costa Murata (Vetulonia) 1963–1979. In P. Rondini & L. Zamboni (Eds.), *Digging up excavations. Processi di ricontestualizzazione di "vecchi" scavi archeologici: Esperienze, problemi e prospettive*. Roma: Edizioni Quasar.

Weaver, I., Meyers, G. E., Mertzman, S. A., Sternberg, R., & Didaleusky, J. (2013). Geochemical evidence for integrated ceramic and roof tile industries at the Etruscan site of Poggio Colla, Italy. *Mediterranean Arhaeology and Archaeometry*, *13*(1), 31–43.

Wentworth, C. K. (1922). A scale of grade and class terms for clastic sediments. *The Journal of Geology*, *30*(5), 377–392. doi: 10.1086/622910.

Winter, N. A. (2002). Commerce in Exile: Terracotta roofing in Etruria, Corfu and Sicily, a Bacchiad family enterprise. *Etruscan Studies*, *9*, 18.

Winter, N. A., Iliopoulos, I., & Ammerman, A. J. (2009). New light on the production of decorated roofs of the 6th c. B.C. at sites in and around Rome. *Journal of Roman Archaeology*, *22*, 6–28. doi: 10.1017/S1047759400020560.